



# $^{99m}\text{Tc}$ -3PRGD<sub>2</sub> SPECT/CT Imaging for Diagnosing Lymph Node Metastasis of Primary Malignant Lung Tumors

Liming Xiao<sup>1</sup>, Shupeng Yu<sup>2</sup>, Weina Xu<sup>2</sup>, Yishan Sun<sup>2</sup>, Jun Xin<sup>2</sup>

<sup>1</sup>Department of Nuclear Medicine, Mianyang Central Hospital, School of Medicine, University of Electronic Science and Technology of China, Mianyang, China

<sup>2</sup>Department of Nuclear Medicine, Shengjing Hospital of China Medical University, Shenyang, China

**Objective:** To evaluate  $^{99m}\text{Tc}$ -three polyethylene glycol spacers-arginine-glycine-aspartic acid ( $^{99m}\text{Tc}$ -3PRGD<sub>2</sub>) single-photon emission computed tomography (SPECT)/computed tomography (CT) imaging for diagnosing lymph node metastasis of primary malignant lung neoplasms.

**Materials and Methods:** We prospectively enrolled 26 patients with primary malignant lung tumors who underwent  $^{99m}\text{Tc}$ -3PRGD<sub>2</sub> SPECT/CT and  $^{18}\text{F}$ -fluorodeoxyglucose ( $^{18}\text{F}$ -FDG) positron emission tomography (PET)/CT imaging. Both imaging methods were analyzed in qualitative (visual dichotomous and 5-point grades for lymph nodes and lung tumors, respectively) and semi-quantitative (maximum tissue-to-background radioactive count) manners for the lymph nodes and lung tumors. The performance of the differentiation of lymph nodes with and without metastasis was determined at the per-lymph node station and per-patient levels using histopathological results as the reference standard.

**Results:** Total 42 stations had metastatic lymph nodes and 136 stations had benign lymph nodes. The differences between metastatic and benign lymph nodes in the visual qualitative and semiquantitative analyses of  $^{99m}\text{Tc}$ -3PRGD<sub>2</sub> SPECT/CT and  $^{18}\text{F}$ -FDG PET/CT were statistically significant (all  $P < 0.001$ ). The area under the receiver operating characteristic curve (AUC) in the semi-quantitative analysis of  $^{99m}\text{Tc}$ -3PRGD<sub>2</sub> SPECT/CT was 0.908 (95% confidence interval [CI], 0.851–0.966), and the sensitivity, specificity, positive predictive value, and negative predictive value were 0.86 (36/42), 0.88 (120/136), 0.69 (36/52), and 0.95 (120/126), respectively. Among the 26 patients (including two patients each with two lung tumors), 15 had pathologically confirmed lymph node metastasis. The difference between primary lung lesions in patients with and without lymph node metastasis was statistically significant only in the semi-quantitative analysis of  $^{99m}\text{Tc}$ -3PRGD<sub>2</sub> SPECT/CT ( $P = 0.007$ ), with an AUC of 0.807 (95% CI, 0.641–0.974).

**Conclusion:**  $^{99m}\text{Tc}$ -3PRGD<sub>2</sub> SPECT/CT imaging may notably perform in the direct diagnosis of lymph node metastasis of primary malignant lung tumors and indirectly predict the presence of lymph node metastasis through uptake in the primary lesions.

**Keywords:**  $^{99m}\text{Tc}$ -3PRGD<sub>2</sub>; SPECT/CT;  $^{18}\text{F}$ -FDG; PET/CT; Lymph node metastasis; Lung cancer

## INTRODUCTION

Malignant lung tumors have the highest mortality rate worldwide [1], and lymph node metastasis is the most

common route of metastasis. Conventional computed tomography (CT) relies mainly on the size of the lymph node to determine metastasis, with the diagnostic criterion being a short-axis diameter of  $> 1$  cm, leading to high false-negative and false-positive rates [2,3]. Recently, positron emission tomography (PET)/CT has demonstrated great value in the diagnosis, staging, treatment, and prognosis of malignant lung tumors [4-6]. However, the examination cost is high, and false-positive uptake of  $^{18}\text{F}$ -fluorodeoxyglucose ( $^{18}\text{F}$ -FDG) in the hilar and mediastinal lymph nodes is common [7]. A non-invasive, cost-effective, and specific imaging method to detect lymph node metastasis is required in clinical practice.

The integrin  $\alpha\text{v}\beta 3$  receptor is a transmembrane

**Received:** May 4, 2023 **Revised:** July 19, 2023

**Accepted:** August 22, 2023

**Corresponding author:** Jun Xin, MD, PhD, Department of Nuclear Medicine, Shengjing Hospital of China Medical University, No. 36 Sanhao Street, Heping District, Shenyang 110004, China

• E-mail: xinj@sj-hospital.org

This is an Open Access article distributed under the terms of the Creative Commons Attribution Non-Commercial License (<https://creativecommons.org/licenses/by-nc/4.0>) which permits unrestricted non-commercial use, distribution, and reproduction in any medium, provided the original work is properly cited.

heterodimer that mediates cell-cell and cell-extracellular matrix adhesions [8,9]. It is ubiquitously present during the development and progression of malignant tumors and is closely associated with angiogenesis and metastasis [8]. This receptor is highly expressed in proliferating tumor cells and activated endothelial cells, but is either not expressed or expressed at very low levels in normal endothelial cells, dormant vascular cells, and other normal cells [10], exhibiting a certain specificity.  $^{99m}\text{Tc}$ -three polyethylene glycol spacers-arginine-glycine-aspartic acid ( $^{99m}\text{Tc}$ -3PRGD<sub>2</sub>) is a single-photon emission computed tomography (SPECT) imaging agent that targets the integrin  $\alpha\text{v}\beta\text{3}$  receptor. Previous studies have confirmed the feasibility of  $^{99m}\text{Tc}$ -3PRGD<sub>2</sub> SPECT imaging for the diagnosis of lung cancer [11], breast cancer [12], esophageal cancer [13], and other malignant tumors and their related lymph node metastases [14,15]. This study aimed to further investigate the performance of  $^{99m}\text{Tc}$ -3PRGD<sub>2</sub> SPECT/CT imaging in the diagnosis of lymph node metastasis in primary malignant lung tumors by comparing it with  $^{18}\text{F}$ -FDG PET/CT imaging.

## MATERIALS AND METHODS

### Ethics Statements

This study was approved by the ethics committee of Shengjing Hospital of China Medical University (approval number: 2020PS06). All enrolled patients provided written informed consents.

### Study Design and Patients

Patients with suspected lung-occupying lesions who were admitted to Shengjing Hospital of China Medical University between August 2020 and February 2021 were prospectively enrolled. The inclusion criteria were as follows: 1) chest CT findings highly suggestive of malignant lung-occupying lesions, with the longest diameter of  $\geq 1.5$  cm and the shortest diameter of  $\geq 1.0$  cm; 2) no prior surgical, invasive procedures, or any related treatments. The exclusion criteria were as follows: 1) CT findings of ground-glass lesions without solid components; 2) unavailable histopathology; 3) pathologically confirmed benign lesions or non-primary lung tumors; and 4) blood glucose not supportive of  $^{18}\text{F}$ -FDG PET/CT imaging and  $^{99m}\text{Tc}$ -3PRGD<sub>2</sub> SPECT/CT imaging. Figure 1 shows a flowchart of the patient enrolment process.

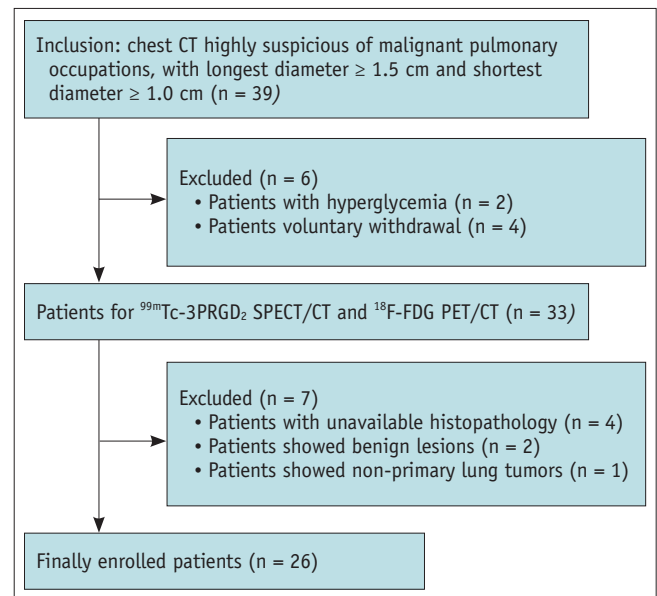


**Fig. 1.** Patient enrollment flowchart. This flowchart shows the study population selection process, including inclusion criteria, and exclusion criteria. CT = computed tomography,  $^{99m}\text{Tc}$ -3PRGD<sub>2</sub> =  $^{99m}\text{Tc}$ -three polyethylene glycol spacer-arginine-glycine-aspartic acid, SPECT = single-photon emission computed tomography,  $^{18}\text{F}$ -FDG =  $^{18}\text{F}$ -fluorodeoxyglucose, PET = positron emission tomography

### Imaging Methods

Patients underwent both  $^{99m}\text{Tc}$ -3PRGD<sub>2</sub> SPECT/CT and  $^{18}\text{F}$ -FDG PET/CT within a brief interval between the two imaging sessions (no more than 1 week).

#### $^{99m}\text{Tc}$ -3PRGD<sub>2</sub> SPECT/CT Imaging

A GE Discovery NM670pro SPECT/CT scanner (GE HealthCare) with a low-energy general-purpose collimator was used with an energy peak of 140 keV and a window width of 20%. Patients were injected intravenously with  $^{99m}\text{Tc}$ -3PRGD<sub>2</sub> at a dose of 11.1 MBq (0.3 mCi)/kg at rest. After 40–50 minutes, anterior and posterior planar scans of the whole body (scan speed: 15–20 cm/min) and chest SPECT scans (matrix, 128 x 128; zoom, 1; 6°/frame; 30 s/frame; 360° imaging) were obtained. Ordered subset expectation maximization was used for SPECT image reconstruction. Low-dose chest CT (120 kV, 80 mA) was performed for anatomical localization and attenuation correction.

#### $^{18}\text{F}$ -FDG PET/CT Imaging

A GE Discovery Elite PET/CT scanner (GE HealthCare) was used. All patients underwent fasting for > 6 hours before the examination, had blood glucose levels < 8.0 mmol/L, and rested for at least 20 minutes in a quiet environment.

The injection dose was 4.44 MBq (0.12 mCi)/kg. Sixty minutes after the injection, a low-dose CT scan (120 kV, 120–240 mA) was performed for attenuation correction. Subsequently, a whole-body  $^{18}\text{F}$ -FDG PET/CT scan was performed to acquire whole-body PET images using the 6–7 bed positions (approximately 90 s/bed position) and reconstructed using a three-dimensional iterative algorithm.

## Image Analysis

### $^{99\text{m}}\text{Tc}$ -3PRGD<sub>2</sub> SPECT/CT and $^{18}\text{F}$ -FDG PET/CT Image Analysis

Image reconstruction and processing for SPECT/CT and PET/CT were performed on Xeleris 4 DR and GE AW4.5 workstations, respectively. Two nuclear medicine physicians separately conducted a blind review of the images, and any discrepancies were resolved through discussion to reach a consensus.

The evaluation of primary lesions in the lung included visual qualitative analysis using a 5-point grading to describe the degree of uptake of the lesion (1, no uptake; 2, uptake lower than the mediastinum; 3, uptake equivalent to the mediastinum; 4, uptake between the mediastinum and liver; and 5, uptake higher than the liver). In a semi-quantitative analysis, the volume of interest (VOI) method was used to obtain the maximum local radioactive count of the lesion. The contralateral lung tissue was used as the control area, and the average radioactive count of the mirrored VOI of the control area was used as the background. The ratio of the maximum lesion VOI count to that of the background (T/B) was calculated.

Individual lymph node stations were evaluated qualitatively and semiquantitatively according to the International Association for the Study of Lung Cancer (IASLC) lymph node map. Visual qualitative analysis classified each lymph node station dichotomously as positive for metastasis if focal prominent well-defined  $^{99\text{m}}\text{Tc}$ -3PRGD<sub>2</sub> uptake compared with mediastinal blood pool activity was found in two or more consecutive transaxial slices. Semi-quantitative analysis was conducted using the same VOI method to obtain the maximum radioactive count of the lymph nodes. The aortic arch area was used as the control area for the lymph nodes and the T/B ratio was calculated. VOI delineation using semi-quantitative analysis is shown in Figure 2.

### Surgery and Pathological Analysis

Surgery was performed within 1 week of imaging. Lymph node dissection was performed routinely during surgery by an experienced thoracic surgeon, who recorded and dissected all visible or palpable lymph nodes within the surgical field, considering all results from preoperative studies, including  $^{99\text{m}}\text{Tc}$ -3PRGD<sub>2</sub> SPECT and  $^{18}\text{F}$ -FDG PET/CT. After surgery, the lymph nodes were separated from the adjacent tissue and assigned specific numbers to indicate their localization of the lymph node. Lung lesions and lymph nodes were fixed in 10% formalin and subsequently embedded in paraffin. Paraffin was cut into 4- $\mu\text{m}$  slices and prepared for routine hematoxylin and eosin staining. Histopathological findings of the lung lesions and lymph nodes served as reference standards.

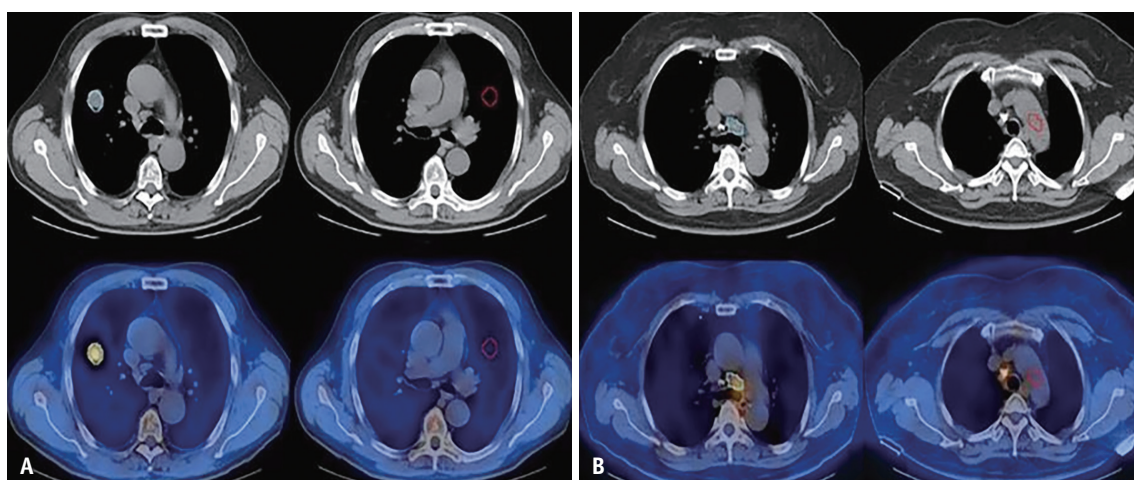


**Fig. 2.** Schematic diagrams of VOI delineation by semi-quantitative analysis. **A:** VOI delineation of a lesion. **B:** VOI delineation of a lymph node. VOI = volume of interest

### Statistical Analysis

Data were analyzed using the MedCalc version 20.0.3 (MedCalc Software bv) and SPSS software (version 26.0; IBM Corp.). Normally distributed data are expressed as the mean ± standard deviation, and non-normally distributed data are expressed as median (25th percentile, 75th percentile). The intraclass correlation coefficient (ICC) was calculated using a two-way random-effects model to test the reproducibility of the semi-quantitative analysis by the two physicians (ICC interpretation: < 0.40, poor; 0.40–0.59, fair; 0.60–0.74, good; ≥ 0.75, excellent). Comparisons between groups were performed using the chi-square test, Fisher’s exact test, independent samples *t*-test, or Mann–Whitney U test. The diagnostic performance of semi-quantitative analysis for lymph node metastasis was determined and compared using the area under the receiver operating characteristic (ROC) curve (AUC) and the DeLong test. Spearman’s correlation coefficient was used to assess the correlation between the uptake of primary lesions and metastatic lymph nodes. A *P*-value of < 0.050 was considered to be statistically significant.

## RESULTS

### Basic Clinical Characteristics of the Patients

In total, 26 patients were enrolled in the present study, including 17 with adenocarcinomas, 8 with squamous cell carcinomas, and 1 with small cell lung carcinoma. Twenty-four patients had a single lesion, and two patients had two lesions (right lung adenocarcinoma), making it a total of 28 lesions. Fifteen patients had metastatic lymph nodes and 11 patients had no metastatic lymph nodes. Based on the IASLC Lymph Node Map, 15 patients with lymph node metastases were pathologically confirmed to have 42 stations with metastatic lymph nodes. Table 1 shows the patient characteristics.

### Identification of Lymph Nodes

The size of metastatic lymph nodes in 42 stations was 0.8 (0.6, 1.3) cm, while the size of benign lymph nodes in 136 stations was 0.5 (0.4, 0.7) cm, and the difference was statistically significant (*P* < 0.001) (Table 1). Based on qualitative visual analysis, most metastatic lymph nodes showed obvious positive uptake on <sup>18</sup>F-FDG PET/CT (32/42) and <sup>99m</sup>Tc-3PRGD<sub>2</sub> SPECT/CT (29/42), whereas some benign lymph nodes showed positive uptake on <sup>18</sup>F-FDG PET/CT (42/136) and <sup>99m</sup>Tc-3PRGD<sub>2</sub> (15/136) (Fig. 3). <sup>18</sup>F-FDG

**Table 1.** Clinical characteristics of the patients and lymph nodes

Clinical characteristic	Values
Patients (n = 26)	
Sex, male:female	13:13
Age, yr	62.6 ± 7.8 (45–76)
Smoking history	
Current smoker	11
Past smoker (quit smoking ≥ 1 years)	6
No smoking history	9
Histopathological type	
ADC	17
SCC	8
SCLC	1
T stage	
T1b	5
T1c	9
T2a	7
T2b	4
T4	1
N stage	
N0	11
N1	4
N2	10
N3	1
TNM stage	
IA	5
IB	4
IIA	2
IIB	3
IIIA	11
IIIB	1
Lymph node stations (n = 178)	
Metastatic:benign	42:136
Size of the tumor, cm	
With metastatic lymph nodes	3.0 (2.4, 3.8)
Without metastatic lymph nodes	3.1 (2.4, 3.8)
Size of the lymph node, cm	
Metastatic lymph nodes	0.8 (0.6, 1.3)
Benign lymph nodes	0.5 (0.4, 0.7)

Data are median (interquartile range) or mean ± standard deviation (range) for continuous variables and numbers of patients or lymph node stations.

ADC = adenocarcinoma, SCC = squamous cell carcinoma, SCLC = small cell lung carcinoma, TNM = tumor node metastasis

PET/CT and <sup>99m</sup>Tc-3PRGD<sub>2</sub> SPECT/CT showed statistically significant differences between metastatic and benign lymph nodes (both *P* < 0.001). In <sup>99m</sup>Tc-3PRGD<sub>2</sub> SPECT/CT, the size of metastatic lymph nodes with positive uptake was 1.0 (0.7, 1.4) cm, and the smallest lymph node was approximately 0.4 cm. Based on semi-quantitative analysis,

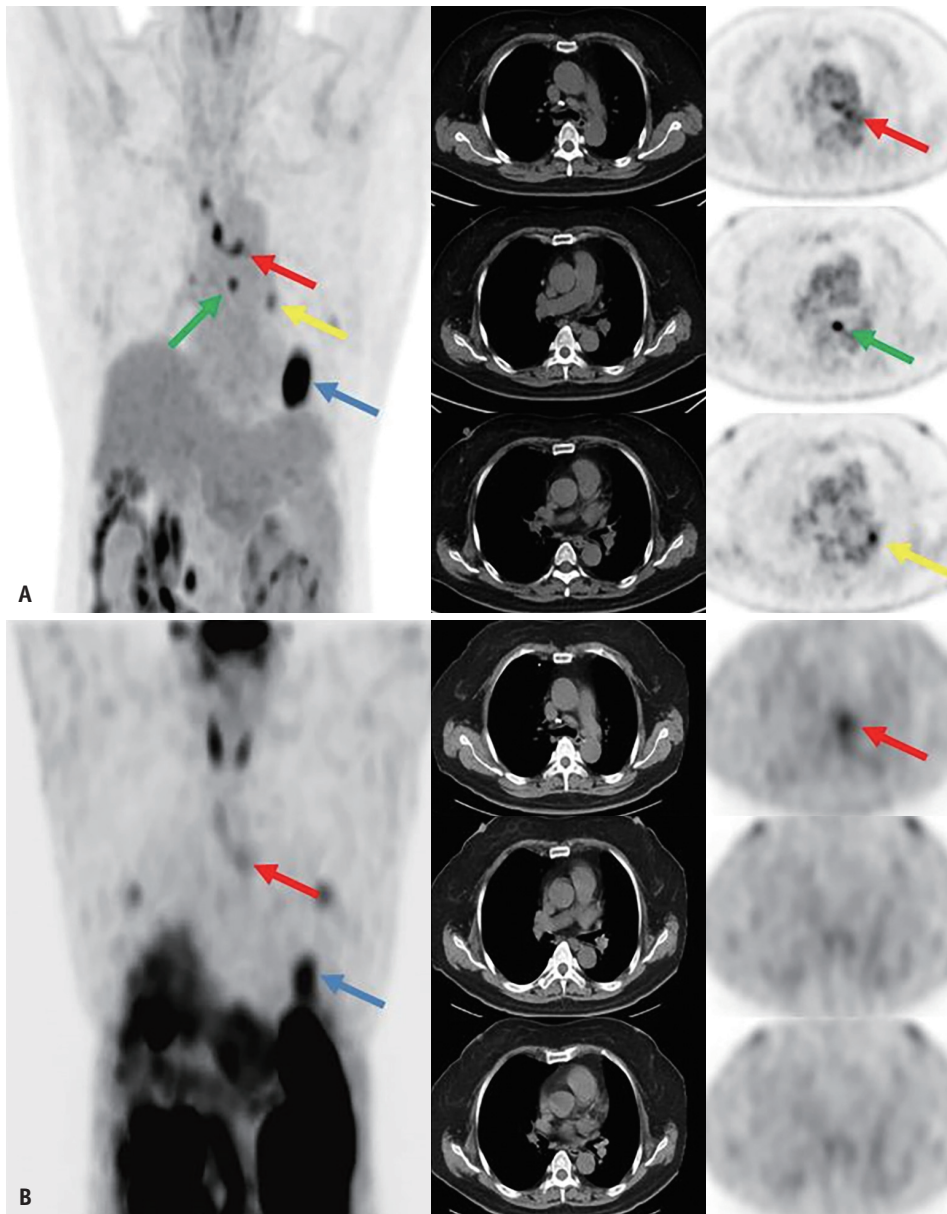


**Fig. 3.**  $^{99m}\text{Tc}$ -3PRGD<sub>2</sub> SPECT/CT and  $^{18}\text{F}$ -FDG PET/CT imaging of metastatic and benign lymph nodes. Positive uptake on  $^{18}\text{F}$ -FDG PET/CT (A) and  $^{99m}\text{Tc}$ -3PRGD<sub>2</sub> SPECT/CT (B) in a 65-year-old female with adenocarcinoma in the left lower lobe (blue arrows) and lymph node metastasis at station 4 L (red arrows). The figures show reactive hyperplasia of the lymph nodes at stations 8 (green arrows) and 11 (yellow arrows), with significant positive uptake on  $^{18}\text{F}$ -FDG PET/CT (A) and no obvious positive uptake on  $^{99m}\text{Tc}$ -3PRGD<sub>2</sub> SPECT/CT (B).  $^{99m}\text{Tc}$ -3PRGD<sub>2</sub> =  $^{99m}\text{Tc}$ -technetium-three polyethylene glycol spacer-arginine-glycine-aspartic acid, SPECT = single-photon emission computed tomography, CT = computed tomography,  $^{18}\text{F}$ -FDG =  $^{18}\text{F}$ -fluorodeoxyglucose, PET = positron emission tomography

the reproducibility of  $^{99m}\text{Tc}$ -3PRGD<sub>2</sub> SPECT/CT (ICC: 0.94) and  $^{18}\text{F}$ -FDG PET/CT (ICC: 0.92) was excellent. For both imaging methods, the T/B values of the metastatic lymph nodes were significantly higher than those of the benign lymph nodes (both  $P < 0.001$ ) (Table 2). The ROC analysis (Fig. 4) showed that the AUC of  $^{99m}\text{Tc}$ -3PRGD<sub>2</sub> SPECT/CT in the semi-quantitative analysis was 0.908 (95% confidence interval [CI], 0.851–0.966), which was significantly higher than

that of  $^{18}\text{F}$ -FDG PET/CT ( $P < 0.001$ ). Diagnostic performance for discriminating lymph node stations with and without metastasis is shown in Table 3.

#### Prediction of Lymph Node Metastasis Through the Uptake in Primary Lung Lesions

Based on visual qualitative analysis, three lesions showed positive uptake (4 points), 25 lesions showed significant

positive uptake (5 points) on <sup>18</sup>F-FDG PET/CT, one lesion showed no obvious uptake (2 points), eight lesions showed positive uptake (4 points), and 19 lesions showed significant positive uptake (5 points) on <sup>99m</sup>Tc-3PRGD<sub>2</sub> SPECT/CT. The uptake in primary lesions on <sup>18</sup>F-FDG PET/CT and <sup>99m</sup>Tc-3PRGD<sub>2</sub> SPECT/CT images showed no statistically significant differences between patients with and without lymph node metastasis ( $P = 0.664$  and  $0.200$ , respectively). In the semi-quantitative analysis, the reproducibility of <sup>99m</sup>Tc-3PRGD<sub>2</sub> SPECT/CT (ICC: 0.94) and <sup>18</sup>F-FDG PET/CT (ICC: 0.97) was excellent. There was no statistically significant difference in the T/B ratio of <sup>18</sup>F-FDG PET/CT in primary lung lesions on between patients with and without lymph node metastasis ( $P = 0.793$ ). Only the T/B ratio of <sup>99m</sup>Tc-3PRGD<sub>2</sub> SPECT/CT showed a statistically significant difference between the two groups ( $P = 0.007$ ). The T/B ratio of primary lung lesions was significantly higher in patients with lymph node metastasis than in those without lymph node metastasis (Table 4). The ROC analysis showed that the AUC for <sup>99m</sup>Tc-3PRGD<sub>2</sub> SPECT/CT in the semi-quantitative analysis was 0.807 (95% CI, 0.641–0.974), with the sensitivity, specificity, and accuracy of 0.88 (15/17), 0.73

(8/11), and 0.82 (23/28), respectively. However, there was no correlation between the T/B ratio of the primary lesions and the metastatic lymph nodes on <sup>99m</sup>Tc-3PRGD<sub>2</sub> SPECT/CT ( $r = -0.219$ ,  $P = 0.217$ ).

**Table 2.** Differences in the semi-quantitative analysis of <sup>99m</sup>Tc-3PRGD<sub>2</sub> SPECT/CT and <sup>18</sup>F-FDG PET/CT of metastatic and benign lymph nodes

T/B ratio	<sup>99m</sup> Tc-3PRGD <sub>2</sub> SPECT/CT	<sup>18</sup> F-FDG PET/CT
Metastatic lymph nodes	2.4 (1.9, 2.9)	3.0 (1.6, 4.6)
Benign lymph nodes	1.3 (1.0, 1.5)	0.8 (1.1, 1.5)
<i>P</i>	< 0.001	< 0.001

Data are median (interquartile range).

<sup>99m</sup>Tc-3PRGD<sub>2</sub> = <sup>99m</sup>technetium-three polyethylene glycol spacers-arginine-glycine-aspartic acid, SPECT = single-photon emission computed tomography, CT = computed tomography, <sup>18</sup>F-FDG = <sup>18</sup>F-fluorodeoxyglucose, PET = positron emission tomography

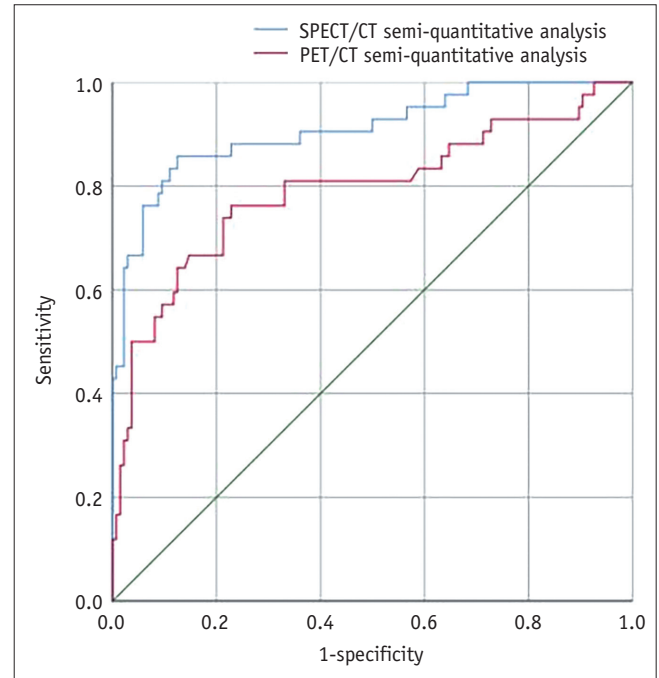


**Fig. 4.** ROC curves for semi-quantitative analysis of <sup>99m</sup>Tc-3PRGD<sub>2</sub> SPECT/CT and <sup>18</sup>F-FDG PET/CT. SPECT/CT semi-quantitative analysis showed significantly better performance than PET/CT semi-quantitative analysis (AUC: 0.908 vs. 0.804;  $P < 0.001$ ). ROC = receiver operating characteristic, <sup>99m</sup>Tc-3PRGD<sub>2</sub> = <sup>99m</sup>technetium-three polyethylene glycol spacers-arginine-glycine-aspartic acid, SPECT = single-photon emission computed tomography, CT = computed tomography, <sup>18</sup>F-FDG = <sup>18</sup>F-fluorodeoxyglucose, PET = positron emission tomography, AUC = area under the receiver operating characteristic curve

**Table 3.** Diagnostic performance for discriminating metastatic and benign lymph nodes with <sup>99m</sup>Tc-3PRGD<sub>2</sub> SPECT/CT and <sup>18</sup>F-FDG PET/CT

Methods	AUC (95% CI)	Cut off	Sensitivity*	Specificity*	Accuracy*	PPV*	NPV*
SPECT/CT visual qualitative analysis	-	-	0.69 (29/42)	0.89 (121/136)	0.84 (150/178)	0.66 (29/44)	0.90 (121/134)
SPECT/CT semi-quantitative analysis	0.908 (0.851, 0.966)	1.70	0.86 (36/42)	0.88 (120/136)	0.88 (156/178)	0.69 (36/52)	0.95 (120/126)
PET/CT visual qualitative analysis	-	-	0.76 (32/42)	0.69 (94/136)	0.71 (126/178)	0.43 (32/74)	0.90 (94/104)
PET/CT semi-quantitative analysis	0.804 (0.715, 0.894)	1.95	0.69 (29/42)	0.86 (117/136)	0.82 (146/178)	0.60 (29/48)	0.90 (117/130)

\*Data in parenthesis are specific quantities of lesions.

<sup>99m</sup>Tc-3PRGD<sub>2</sub> = <sup>99m</sup>technetium-three polyethylene glycol spacers-arginine-glycine-aspartic acid, SPECT = single-photon emission computed tomography, CT = computed tomography, <sup>18</sup>F-FDG = <sup>18</sup>F-fluorodeoxyglucose, PET = positron emission tomography, AUC = area under the receiver operating characteristic curve, CI = confidence interval, PPV = positive predictive value, NPV = negative predictive value

**Table 4.** Differences in the semi-quantitative analysis of  $^{99m}\text{Tc}$ -3PRGD<sub>2</sub> SPECT/CT and  $^{18}\text{F}$ -FDG PET/CT for primary lung lesions in patients with and without metastatic lymph nodes

T/B ratio of primary lung tumor	$^{99m}\text{Tc}$ -3PRGD <sub>2</sub> SPECT/CT	$^{18}\text{F}$ -FDG PET/CT
Patient with lymph node metastasis	12.2 (9.4, 15.5)	27.0 ± 9.4
Patient without lymph node metastasis	8.2 (7.1, 11.0)	28.1 ± 13.0
<i>P</i>	0.007	0.793

Data are median (interquartile range) or mean ± standard deviation (range).

$^{99m}\text{Tc}$ -3PRGD<sub>2</sub> =  $^{99m}\text{Tc}$ -technetium-three polyethylene glycol spacers-arginine-glycine-aspartic acid, SPECT = single-photon emission computed tomography, CT = computed tomography,  $^{18}\text{F}$ -FDG =  $^{18}\text{F}$ -fluorodeoxyglucose, PET = positron emission tomography

## DISCUSSION

Lymph node dissection for malignant lung tumors is an important but controversial topic. Systematic mediastinal and hilar lymph node dissections have been advocated [16]. However, systematic lymph node dissection has certain shortcomings, mainly manifesting as the large scope of lymph node dissection, increased trauma, and postoperative complications. Helping clinicians more accurately determine lymph node staging and develop treatment plans remains an urgent challenge. A previous study [14] established the feasibility of  $^{99m}\text{Tc}$ -3PRGD<sub>2</sub> SPECT/CT imaging for the diagnosis of lymph node metastasis in non-small cell lung cancers. Building on this, the current study explored the diagnostic value both of visual qualitative and semi-quantitative analyses of  $^{99m}\text{Tc}$ -3PRGD<sub>2</sub> SPECT/CT imaging in assessing lymph node metastasis from aspects of the lymph nodes and lymph node metastasis of malignant lung tumors.

In differentiating lymph node properties,  $^{99m}\text{Tc}$ -3PRGD<sub>2</sub> SPECT/CT imaging exhibited exceptional diagnostic efficacy, particularly when using semiquantitative analysis, where the AUC reached 0.908, which was significantly higher than that of  $^{18}\text{F}$ -FDG PET/CT. All diagnostic parameters were high, satisfying the clinical application needs. Unlike  $^{18}\text{F}$ -FDG PET/CT, which often results in false-positive uptake in the mediastinal and hilar lymph nodes [7],  $^{99m}\text{Tc}$ -3PRGD<sub>2</sub> SPECT/CT demonstrates a lower false-positive rate and greater specificity. Notably, the specificity of  $^{99m}\text{Tc}$ -3PRGD<sub>2</sub> SPECT/CT using the simple and commonly used visual analysis method was 0.89, whereas that of  $^{18}\text{F}$ -FDG PET/CT visual analysis was only 0.69, demonstrating a significant advantage over  $^{18}\text{F}$ -FDG PET/CT. This characteristic may be attributed to the

tumor-specific nature of  $^{99m}\text{Tc}$ -3PRGD<sub>2</sub> as an imaging agent [10], enabling more accurate differentiation of malignant tumor metastatic foci from certain benign lesions, such as active tuberculosis, proliferative granulomas, sarcoidosis, and reactive hyperplasia.  $^{99m}\text{Tc}$ -3PRGD<sub>2</sub> SPECT/CT can help stage lymph nodes in malignant lung tumors more precisely than  $^{18}\text{F}$ -FDG PET/CT and can determine the extent of surgical lymph node dissection, reducing the need for invasive procedures and extensive surgery-related adverse effects. This modality may offer new opportunities to assist patients with malignant lung tumors in decision-making regarding surgical approaches and treatment plans.

Another advantage of  $^{99m}\text{Tc}$ -3PRGD<sub>2</sub> SPECT/CT is its ability to predict the presence of lymph node metastasis based on the uptake of the primary lesion in the lung with high predictive performance. The uptake of  $^{99m}\text{Tc}$ -3PRGD<sub>2</sub> in primary lung lesions with metastatic lymph nodes is significantly higher than in those without metastasis, suggesting that primary lung lesions with metastatic lymph nodes may have higher integrin  $\alpha\beta 3$  receptor expression. The high expression of the integrin  $\alpha\beta 3$  receptor and increased uptake of  $^{99m}\text{Tc}$ -3PRGD<sub>2</sub> in primary lesions may indicate a higher tumor activity and invasiveness [17,18]. However, we observed that the uptake by the primary lesions and metastatic lymph nodes was not correlated. The uptake of  $^{99m}\text{Tc}$ -3PRGD<sub>2</sub> in primary lung lesions may be a potential parameter for determining lymph node metastasis and may serve as a supplementary and indirect evidence for the identification of lymph node properties in malignant lung tumors using  $^{99m}\text{Tc}$ -3PRGD<sub>2</sub> SPECT/CT imaging, contributing to the improved ability of  $^{99m}\text{Tc}$ -3PRGD<sub>2</sub> SPECT/CT imaging for lymph node staging of malignant lung tumors.

Moreover, compared with previous molecular probes of a similar nature,  $^{99m}\text{Tc}$ -3PRGD<sub>2</sub> offers greater convenience and faster probe preparation, along with rapid blood clearance and exceptionally high safety [19,20]. Adverse reactions occur infrequently, and the use of SPECT/CT imaging systems offers improved cost-effectiveness and broader accessibility than PET/CT.

This study had several limitations. First, the sample size was small and consisted of the same types of lymph nodes with a notably smaller number of metastatic lymph nodes than benign ones, which may have resulted in biased statistical outcomes. The advantage of predicting metastatic characteristics based on  $^{99m}\text{Tc}$ -3PRGD<sub>2</sub> uptake in primary lung lesions requires confirmation using larger sample sizes. Second, the low spatial resolution of SPECT/CT equipment, considerable

attenuation and scatter effects, and incomplete matching of scan sequences contribute to the diminished image quality. This complicates the visual diagnosis for some lymph nodes and might be a major factor behind the significantly lower sensitivity of visual analysis compared to semi-quantitative analysis. Moreover, we did not group patients according to lymph node size, which will be refined in subsequent studies. Finally, although two nuclear medicine physicians delineated and calibrated the primary lesions and lymph nodes, accurate measurement of some lesions and lymph nodes proved challenging because of the physiological uptake interference from blood vessels and the esophagus, potentially introducing bias into the experimental results.

In conclusion, <sup>99m</sup>Tc-3PRGD<sub>2</sub> SPECT/CT imaging demonstrated notable diagnostic performance in discerning the nature of lymph nodes in patients with primary malignant lung tumors, particularly with its high specificity. Furthermore, it has the potential to indirectly predict the presence or absence of lymph node metastasis through its uptake by primary lung lesions.

#### Availability of Data and Material

The datasets generated or analyzed during the study are available from the corresponding author on reasonable request.

#### Conflicts of Interest

The authors have no potential conflicts of interest to disclose.

#### Author Contributions

Conceptualization: Liming Xiao, Jun Xin. Data curation: Liming Xiao. Formal analysis: Liming Xiao, Jun Xin. Investigation: Liming Xiao, Shupeng Yu, Weina Xu. Methodology: Liming Xiao, Shupeng Yu, Weina Xu, Yishan Sun. Project administration: Liming Xiao, Jun Xin. Resources: Liming Xiao, Jun Xin. Software: Liming Xiao, Yishan Sun. Supervision: Jun Xin. Validation: Jun Xin. Writing—original draft: Liming Xiao. Writing—review & editing: all authors.

#### ORCID IDs

Liming Xiao

<https://orcid.org/0009-0002-1227-6162>

Shupeng Yu

<https://orcid.org/0009-0004-1327-0306>

Weina Xu

<https://orcid.org/0009-0006-1990-3930>

Yishan Sun

<https://orcid.org/0000-0001-7891-2104>

Jun Xin

<https://orcid.org/0000-0001-5660-6368>

#### Funding Statement

None

#### Acknowledgments

The authors thank all their coworkers involved in the study for their support and assistance.

#### REFERENCES

1. Siegel RL, Miller KD, Wagle NS, Jemal A. Cancer statistics, 2023. *CA Cancer J Clin* 2023;73:17-48
2. Kudo S, Imai K, Ishiyama K, Hashimoto M, Saito H, Motoyama S, et al. New CT criteria for nodal staging in non-small cell lung cancer. *Clin Imaging* 2014;38:448-453
3. Xia Y, Zhang B, Zhang H, Li W, Wang KP, Shen H. Evaluation of lymph node metastasis in lung cancer: who is the chief justice? *J Thorac Dis* 2015;7(Suppl 4):S231-S237
4. Liao X, Liu M, Li S, Huang W, Guo C, Liu J, et al. The value on SUV-derived parameters assessed on 18F-FDG PET/CT for predicting mediastinal lymph node metastasis in non-small cell lung cancer. *BMC Med Imaging* 2023;23:49
5. Marcus C, Tajmir SH, Rowe SP, Sheikhabaehi S, Solnes LB. 18F-FDG PET/CT for response assessment in lung cancer. *Semin Nucl Med* 2022;52:662-672
6. Sun Y, Xiao L, Wang Y, Liu C, Cao L, Zhai W, et al. Diagnostic value of dynamic 18F-FDG PET/CT imaging in non-small cell lung cancer and FDG hypermetabolic lymph nodes. *Quant Imaging Med Surg* 2023;13:2556-2567
7. Billé A, Pelosi E, Skanjeti A, Arena V, Errico L, Borasio P, et al. Preoperative intrathoracic lymph node staging in patients with non-small-cell lung cancer: accuracy of integrated positron emission tomography and computed tomography. *Eur J Cardiothorac Surg* 2009;36:440-445
8. Xiao L, Xin J. Advances in clinical oncology research on <sup>99m</sup>Tc-3PRGD<sub>2</sub> SPECT imaging. *Front Oncol* 2022;12:898764
9. Serini G, Valdembri D, Bussolino F. Integrins and angiogenesis: a sticky business. *Exp Cell Res* 2006;312:651-658
10. Niu G, Chen X. Why integrin as a primary target for imaging and therapy. *Theranostics* 2011;1:30-47
11. Zhu Z, Miao W, Li Q, Dai H, Ma Q, Wang F, et al. <sup>99m</sup>Tc-3PRGD<sub>2</sub> for integrin receptor imaging of lung cancer: a multicenter study. *J Nucl Med* 2012;53:716-722
12. Chen Z, Fu F, Li F, Zhu Z, Yang Y, Chen X, et al. Comparison of [<sup>99m</sup>Tc]3PRGD<sub>2</sub> imaging and [18F]FDG PET/CT in breast cancer and expression of integrin αvβ3 in breast cancer vascular endothelial cells. *Mol Imaging Biol* 2018;20:846-856
13. Zheng S, Chen Z, Huang C, Chen Y, Miao W. [<sup>99m</sup>Tc]3PRGD<sub>2</sub>

- for integrin receptor imaging of esophageal cancer: a comparative study with [18F]FDG PET/CT. *Ann Nucl Med* 2019;33:135-143
14. Jin X, Liang N, Wang M, Meng Y, Jia B, Shi X, et al. Integrin imaging with 99mTc-3PRGD2 SPECT/CT shows high specificity in the diagnosis of lymph node metastasis from non-small cell lung cancer. *Radiology* 2016;281:958-966
  15. Lv N, Gao S, Bai L, Ji B, Xue J, Ge X, et al. Advantages of 99mTc-3PRGD2 SPECT over CT in the preoperative assessment of lymph node metastasis in patients with esophageal cancer. *Ann Nucl Med* 2019;33:39-46
  16. Watanabe S. Lymph node dissection for lung cancer: past, present, and future. *Gen Thorac Cardiovasc Surg* 2014;62:407-414
  17. Felding-Habermann B, Fransvea E, O'Toole TE, Manzuk L, Faha B, Hensler M. Involvement of tumor cell integrin  $\alpha\beta3$  in hematogenous metastasis of human melanoma cells. *Clin Exp Metastasis* 2002;19:427-436
  18. Li M, Wang Y, Li M, Wu X, Setrerrahmane S, Xu H. Integrins as attractive targets for cancer therapeutics. *Acta Pharm Sin B* 2021;11:2726-2737
  19. Shi J, Wang L, Kim YS, Zhai S, Liu Z, Chen X, et al. Improving tumor uptake and excretion kinetics of 99mTc-labeled cyclic arginine-glycine-aspartic (RGD) dimers with triglycine linkers. *J Med Chem* 2008;51:7980-7990
  20. Jia B, Liu Z, Zhu Z, Shi J, Jin X, Zhao H, et al. Blood clearance kinetics, biodistribution, and radiation dosimetry of a kit-formulated integrin  $\alpha\beta3$ -selective radiotracer 99mTc-3PRGD 2 in non-human primates. *Mol Imaging Biol* 2011;13:730-736